MIZMAS: Modeling the Evolution of Ice Thickness and Floe Size Distributions in the Marginal Ice Zone of the Chukchi and Beaufort Seas

Jinlun Zhang
Applied Physics Laboratory, University of Washington
1013 NE 40th St
Seattle, WA 98105
phone: (206) 543-5569 fax: (206) 616-3142 email: zhang@apl.washington.edu

Axel Schweiger
Applied Physics Laboratory, University of Washington
1013 NE 40th St
Seattle, WA 98105
phone: (206) 543-1312 fax: (206) 616-3142 email: axel@apl.washington.edu

Michael Steele
Applied Physics Laboratory, University of Washington
1013 NE 40th St
Seattle, WA 98105
phone: (206) 543-6586 fax: (206) 616-3142 email: mas@apl.washington.edu

Grant Number: N00014-12-1-0112

LONG-TERM GOALS

Our long-term goal is to develop a robust, high-resolution coupled sea ice–ocean modeling and assimilation system that is capable of accurately predicting sea ice conditions in the marginal ice zone (MIZ) of the Chukchi and Beaufort seas (CBS) on seasonal time scales. Our primary interest is the ability to realistically simulate the evolution of the multicategory ice thickness and floe size distributions (ITD, FSD) jointly in the CBS MIZ. Particularly, we would like to improve model physics to represent changes in FSD due to ice advection, thermodynamic growth or decay, lateral melting, ridging and rafting, and wave-induced fragmentation through theoretical development and numerical implementation.

OBJECTIVES

Our main scientific objectives are to:

(1) Examine the historical evolution of the CBS MIZ ice–ocean system and its ITD and FSD from 1978 to the present to quantify and understand the large-scale changes that have occurred in the system.

(2) Identify key linkages and interactions among the atmosphere, sea ice, and ocean, to enhance our understanding of mechanisms affecting the CBS MIZ dynamic and thermodynamic processes.

(3) Explore the predictability of the seasonal evolution of the MIZ and the summer location of the ice edge in the CBS through seasonal ensemble forecast.

(4) Explore the impacts of future anthropogenic global climate change (including a summer arctic ice-free regime) on the CBS MIZ processes through downscaling future projection simulations.

APPROACH

To address the scientific objectives, we plan to develop, implement, and validate a new coupled ice–ocean **M**arginal **I**ce **Z**one **M**odeling and **A**ssimilation **S**ystem (**MIZMAS**) that will enhance the representation of the unique MIZ processes by incorporating a FSD and corresponding model improvements. A successful incorporation of a FSD will allow MIZMAS to simulate the evolution of both ITD and FSD at the same time. The development of MIZMAS will be based on systematic model parameterization, calibration, and validation, and data assimilation, taking advantage of the integrated observational and modeling efforts planned by the ONR MIZ research initiative. Meanwhile, we also uses the **P**an-arctic **I**ce/**O**cean **M**odeling and **A**ssimilation **S**ystem (**PIOMAS**), a variant of MIZMAS, to study changes in the Arctic sea ice and ocean system. With a coarser model resolution than MIZMAS, PIOMAS is more computationally efficient in process studies. Jinlun Zhang, Axel Schweiger, Mike Steele at the University of Washington are investigators of this project. Harry Stern at UW also helped in analyzing satellite images of sea ice floes and deriving FSD. In addition, an undergraduate student at UW, Margaret Stark, continued to work on processing and analyzing satellite images of sea ice this year. A programmer at APL, K. Runciman, also helped in comparing MIZMAS results with observations from ice-tethered profilers, and autonomous gliders.

WORK COMPLETED

We developed a FSD theory that is coupled to the ITD theory of Thorndike et al. (1975) in order to explicitly simulate the evolution of FSD and ITD jointly. The FSD theory includes a FSD function and a FSD conservation equation in parallel with the ITD equation. We tested the numerical implementation of the FSD equation in an idealized sea ice model. We also tested model sensitivity to different partitions of floe size categories for calculating FSD. The FSD theory and the results from the idealized sea ice model were published in J. Geophysical Research (Zhang et al., 2015).

We were able to incorporate the FSD theory into PIOMAS, a dynamic thermodynamic sea ice model that also simulates 12-category ITD. The expanded PIOMAS simulates a FSD that includes 12 categories of ice floes with caliper diameters ranging from 0.1 m to ~3000 m. We have been using the new PIOMAS to examine the realistically simulated seasonal evolution of FSD and preparing a manuscript for possible publication in the near future.

To support the planning of the ONR MIZ filed work in 2014, we developed an ensemble seasonal forecast system for predicting Arctic sea ice weeks to months in advance using MIZMAS that has high-resolution coverage for the CBS. In 2015, we continued to conduct ensemble seasonal forecast monthly in an effort to support other ONR field work such as the Sea State program. To obtain the "best possible" initial ice-ocean conditions for the forecast, a hindcast was conducted, which assimilates satellite ice concentration and sea surface temperature data (see Zhang et al., 2008). We developed a web page to make it easier to access the hindcast and forecast results as soon as available (http://psc.apl.uw.edu/research/projects/mizmas/hindcast-and-forecast/).

To support the ONR MIZ field work after the clusters of instruments were deployed in March 2014, we developed a numerical framework for 48 hour forecast of sea ice thickness and drift in and around the Beaufort Sea MIZ using MIZMAS. The short-term sea ice forecast system was forced by the forecast atmospheric data from the NCEP (National Center for Environmental Prediction) Climate Forecast System version 2 (CFSv2). The forecast system was used to predict ice thickness in the Beaufort Sea MIZ 48 hours in advance, focusing on the areas around the five clusters. It was also used to predict the movement of these clusters. We did the forecast almost every work day from July 21, 2014 onward, when the instruments were taking measurements in the Beaufort Sea. The results from this work were analyzed in a manuscript that has been submitted to J. Geophysical Research (Schweiger and Zhang, 2015).

We continued to develop procedures for extracting FSD from satellite images. Our work focuses on the extraction of FSD from NASA/MODIS (pixel size 250 meters) and USGS/Global Fiducials Library (GFL) (pixel size 1 meter). We continued to seek to establish a relationship between the FSD at the large scale and the small scale, enabling us to parameterize the important but difficult-to-observe small-scale FSD in terms of the large-scale FSD. Landsat optical images at 15m resolution are used as well. Our projec establishes a database of temporally and spatially varying FSD in the Beaufort Sea from 2013 through 2014 that will be suitable for model initialization and validation. In addition to our analysis based on optical sensors, we are collaborating with others (e.g. Phil Huang) who are focusing on SAR-derived FSD to complement the approaches and integrate the results. The sattelite derived FSD database has been very helpful for model calibration and validation.

We conducted extensive MIZMAS calibration and validation using a range of ocean temperature and salinity observations in the CBS, including those from the SIZRS AXCTD, ice-tethered profilers, UpTempO buoys, and autonomous gliders, supported by ONR. We performed numerous MIZMAS runs from 1970 to 2014 in order to reduce model misfit as much as possible. We are now analyzing the calibrated model results over the period 1979–2014 to examine the variability of the Beaufort Sea near surface temperature maximum (NSTM), the Pacific Water layers, and the distribution of halocline water masses in response to the Beaufort Gyre spin-up.

We investigated forcing mechanisms for seasonal ice loss in the Beaufort Sea in 2014 (Steele et al., 2015). In 2015, we continued to explore the possibility of predicting the seasonal ice retreat there months in advance and obtained some new results.

We have been collaborating with Drs. W. Wang and T. Collow at the NOAA Center for Weather and Climate Prediction to improve seasonal forecast of Arctic sea ice using NOAA's Climate Forecast System version 2 (CFSv2) initialized with PIOMAS sea ice thickness fields. We have been providing PIOMAS sea ice thickness fields for the days 8–12 each month to the CFSv2 as initial sea ice thickness conditions. Results from this collaboration have been distributed to NOAA field offices and also submitted to Monthly Weather Review (Collow et al., 2015).

We collaborated with Dr. E. Blanchard-Wrigglesworth at the University of Washington to study model skill and sensitivity to initial conditions in an operational sea ice prediction system. Results from this collaboration have been submitted to Geophysical Research Letters (Blanchard-Wrigglesworth et al., 2015).

RESULTS

Modeling:

A FSD theory is developed and coupled to the ITD theory of *Thorndike et al*. (1975) in order to explicitly simulate the evolution of FSD and ITD jointly. The FSD theory includes a FSD function and a FSD conservation equation in parallel with the ITD equation. The FSD equation takes into account changes in FSD due to ice advection, thermodynamic growth, and lateral melting. It also includes changes in FSD because of mechanical redistribution of floe size due to ice ridging and, particularly, ice fragmentation induced by stochastic ocean surface waves. The FSD theory is implemented in PIOMAS, a coupled sea ice and ocean modeling and assimilation system. After the implementation, PIOMAS is able to simulate 12-category ITD and 12-category FSD jointly. Model results show that the simulated cumulative FSD follows a power law in space and time as observed by satellites and airborne surveys (Figure 1). The simulated values of the exponent of the power law are also in the range of the MODIS observations, with mean model bias of –0.03 and model-observation correlation of 0.57 (Figure 2). This indicates that the model is able to capture 32% of the variance of the satellite derived power-law exponent.

Figure 1 further shows that the simulated cumulative FSD at the high end of the floe size range often deviates from a power law by showing a steeper decent (e.g., the red and pink colors for August and September). This is a normal model outcome because of decreasing number, and ultimately disappearance, of floes of large sizes as ice continues to break and melt in summer. The falloff from a power law at the high end is often seen in observations and described by an upper truncated power law. Here the upper truncated power law is replicated in the model.

It is found that floe size redistribution and the resulting FSD and mean floe size do not depend on how floe size categories are numerically partitioned over a given floe size range (Figure 3), suggesting the robustness of the FSD theory. The ability to explicitly simulate multicategory FSD and ITD together may help to incorporate additional model physics, such as FSD-dependent ice mechanics, surface exchange of heat, mass, and momentum, and wave-ice interactions.

We found that MIZMAS is able to realistically simulate the seasonal evolution of salinity and temperature profiles in the Beaufort Sea in comparison with ITP observations (Figure 4). For this particular comparison, the model shows a tendency to somewhat overestimate salinity at the surface and underestimate it below the surface layer, but it well captures the summer freshening in the upper ocean due to ice melt. The model is able to reproduce the formation of the observed near surface temperature maximum (NSTM) in summer, however the simulated NSTM is greater than the observed. This may be due in part to the fact that the ITP measurements were taken under ice, while model results are averages over both ice and open water areas. The model is also able to realistically simulate the temperature distribution of the warm Pacific Water layer, with generally small positive or negative biases (Figure 4).

MIZMAS ice drift forecasts are assessed through comparisons with observed IABP buoy drifts and drift forecasts made using climatological ice velocities. We found that the forecast drift positions have an RMS error of 6 km after 24 hours compared with a 12 km error for climatological forecasts (using long-term daily mean ice drifts), a 50% reduction in error. Position forecasts remain skillful relative to climatology at 8-days from the initial forecast with RMS positions errors in the order of 45 km (Figure 5).

Remote Sensing:
MODIS images are downloaded automatically from the NASA Global Imagery Browse Service via the Web Map Service interface. Cloud-free regions in the images are delineated manually based on visible and near-infrared bands 3–6–7. We have processed 256 images, over 187 days for the period March–October, 2013–2014, in the Beaufort Sea region. The median size of the cloud-free regions is about 80,000 km^2. A low-pass filter (Gaussian) with length scale 25 km is applied to a cloud-free region (red in Figure 4a and full view in Figure 4b), and the smoothed image is subtracted from the original image. Positive differences are assigned a value 1 (ice); negative differences are assigned a value 0 (water). This creates a binary image. After that, a morphological *erosion* operation is applied to the binary image in order to separate ice floes that are touching. Floes in the resulting eroded image are labeled using a recursive algorithm that identifies groups of connected pixels. Floes are then "re-grown" outward using a variation of the morphological *dilation* operation in which only those pixels that were originally assigned as ice are allowed to re-grow. Properties of each floe are then easily calculated, such as area, perimeter, and caliper diameter. This allows us to obtain the number density, which is defined as the number of floes of a given size within the cloud-free region divided by the area of the region. The number density is one way to express the FSD. The advantage of MODIS images is the ability to derive FSD with much better spatial and temporal sampling than currently possible with high resolution images. However, physically more imporatent floes at the smaller scale can not be directly derived because of the 250 m sensor resolution. Sine FSD is proposed to follow a power law, smaller scale FSD can be derived indirectly by extrapolationg the slope of the FSD derived at the MODIS scale. To test this assumption, we compared the FSD derived from MODIS to FSD derived from an spatially overlapping high resolution MEDEA image (1 m resolution). The images were separated by 3 days. The MEDEA image was manually digitized and 6000 floes extracted. The comparison is shown in Figure 6. The MODIS FSD is slightly steeper (–2.4) than the FSD derived from the MEDEA image. A larger number of comparisons will be done in the future.

Using the method described above, we have been able derive FSD from satellite for the 2013 and 2014 season. Figure 7 shows the location of images during 2014 and the derived seasonal cycle. The seasonal cycle of the slope of the FSD ranges from –2.0 in March to –2.8 in August indicating an increase in the number of smaller floes over the course of the melt season.

Changes in Sea Ice in the Beaufort Sea:
We studied sea ice changes in the Beaufort Sea over the past decades. We found that seasonal ice loss is generally late in the western Beaufort owing to advection of old, thick ice from the northeast, but this is trending toward earlier dates as thick ice has recently thinned. Meanwhile, ice loss is early in the eastern Beaufort owing to easterly winds in spring, and this has not changed over time. The result is that seasonal ice loss is becoming more synchronous (i.e., more zonally uniform) across the Beaufort Sea. This holds for the Date of ice Retreat (DOR, defined as the final day when concentration falls below 15%) although with less statistical significance relative to the Date of ice Opening (DOO, defined as the final day of the spring/summer when ice concentration falls below 80%) (Steele et al., 2015).

In this past year, we extended our predictability analysis for 2013–2015, and found good correlation between the strength of spring easterly winds and the DOR in the eastern Beaufort Sea. The mean DOR in this region is early July (Steele et al., 2015, Figure 12), so this gives 2–3 months of predictive lead time, on average. Figure 8 shows that predictability improves as the linear relationship is trained over more years (i.e., in later years). Predictions also improve when averaging over more days in spring (i.e., using 2 months instead of just 1 month). The prediction bias is quite low (0–3 days) for all

three of our predictors (u_{April}, u_{May}, u_{AprMay}), and the root mean square error (RMSE) is 2–3 weeks, with correlations of ~ 0.5. We plan to use this technique in the 2016 SIPN (Sea Ice Prediction Network) forecasting challenge.

IMPACT/APPLICATIONS

The objectives of this project address directly some of the key questions raised in the ONR MIZ research initiative: ***Emerging Dynamics of the Marginal Ice Zone***. These questions are explored by modeling, analyzing, and understanding the large-scale changes that have occurred in the CBS MIZ, and by assessing the possible changes that lie ahead. Aiming to improve our understanding of the CBS MIZ processes, interactions, and feedbacks, this ONR MIZ research contributes to the inter-agency Study of Environmental Arctic Change (SEARCH). Aiming to enhance model physics, this research addresses the U.S. Navy's needs to improve the predictability of sea ice in the region. A successful development of MIZMAS will mark a new sea ice model that is able to explicitly simulate the evolution of multicategory ice thickness and floe size distributions simultaneously. The theoretical and numerical work on FSD will provide a foundation to improve significantly the representation of key MIZ processes. This will be a significant step forward towards developing the next generation of sea ice models for use in operational forecast and climate predictions.

RELATED PROJECTS

Supported by NASA and in collaboration with Drs. Carin Ashjian, Robert Campbell, Victoria Hill, Yvette Spitz, Zhang and Steele are investigating planktonic ecosystem response to changing sea ice and upper ocean physics in the CBS. We are modeling the integrated system of sea ice, ocean, and marine ecosystem in the CBS (http://psc.apl.washington.edu/zhang/Chukchi_Beaufort/model.html).

REFERENCES

Thorndike, A.S., D.A. Rothrock, G.A. Maykut, and R. Colony (1975), The thickness distribution of sea ice. *J. Geophys. Res.*, *80*, 4501–4513.

Zhang, J., M. Steele, R.W. Lindsay, A. Schweiger, and J. Morison, Ensemble one-year predictions of arctic sea ice for the spring and summer of 2008. *Geophys. Res. Lett.*, *35*, L08502, doi:10.1029/2008GL033244, 2008.

PUBLICATIONS

Blanchard-Wrigglesworth, E., R. Cullather, W. Wang, J. Zhang, and C.M. Bitz, Model skill and sensitivity to initial conditions in an operational sea ice prediction system, *Geophys. Res. Lett.*, *submitted*, 2015 [accepted, refereed].

Laxon, W.S, K. A. Giles, A. L. Ridout, D. J. Wingham, R. W., R.Cullen, R. Kwok, A. Schweiger, J. Zhang, C. Haas, S. Hendricks, R. Krishfield, N. Kurtz, S Farrell, M Davidson, CryoSat-2 estimates of Arctic sea ice thickness and volume, *Geophys. Res. Lett.*, doi:10.1002/grl.5019, 2013 [published, refereed].

Lindsay, R., C. Haas, S. Hendricks, P. Hunkeler, N. Kurtz, J. Paden, B. Panzer, J. Sonntag, J. Yungel, and J. Zhang, Seasonal forecasts of arctic sea ice initialized with observations of ice thickness, *Geophys. Res. Lett.*, *39*, L21502, doi:10.1029/2010GL053576, 2012 [published, refereed].

Lindsay, R., M. Wensnahan, A. Schweiger, and J. Zhang, Evaluation of seven different atmospheric reanalysis products in the Arctic, *J. Climate*, *27*, 2588-2606, doi: http://dx.doi.org/10.1175/JCLI-D-13-00014.s1, 2014 [published, refereed].

Martin, T., M. Steele, and J. Zhang, Seasonality and long-term trend of Arctic Ocean surface stress in a model, *J. Geophy. Res*., *119*, 1723-1738, doi:10.1002/2013JC009425, 2014 [published, refereed].

Miller, R. L., G. A. Schmidt, L. S. Nazarenko, N. Tausnev, R. Ruedy, M. Kelley, K. K. Lo, I. Aleinov, M. Bauer, S. Bauer, R. Bleck, V. Canuto, Y. Cheng, T. L. Clune, A. DelGenio, G. Faluvegi, J. E. Hansen, R. J. Healy, N. Y. Kiang, D. Koch, A. A. Lacis, A. N. LeGrande, J. Lerner, J. Marshall, S. Menon, V. Oinas, J. Perlwitz, M. J. Puma, D. Rind, A. Romanou, G. L. Russell, M. Sato, D. T. Shindell, S. Sun, K. Tsigaridis, N. Unger, A. Voulgarakis, M.-S. Yao, and J. Zhang, CMIP5 historical simulations (1850-2012) with GISS ModelE2. *J. Advances in Modeling Earth Systems, 6*, no. 2, 441-477, doi:10.1002/2013MS000266, 2014 [published, refereed].

Nazarenko, L.S., G. A. Schmidt, R.L. Miller, N. Tausnev, M. Kelley, R. Ruedy, G.L. Russell, I. Aleinov, M. Bauer, S. Bauer, R. Bleck, V. Canuto, Y. Cheng, T. L. Clune, A. DelGenio, G. Faluvegi, J. E. Hansen, R. J. Healy, N. Y. Kiang, D. Koch, A. A. Lacis, A. N. LeGrande, J. Lerner, K. K. Lo, S. Menon, V. Oinas, J. Perlwitz, M. J. Puma, D. Rind, A. Romanou, M. Sato, D. T. Shindell, S. Sun, K. Tsigaridis, N. Unger, A. Voulgarakis, M.-S. Yao, and J. Zhang, Future Climate Change under RCP Emission Scenarios with the GISS ModelE2, *J. Advances in Modeling Earth Systems*, 2013 [submitted, refereed].

Peralta-Ferriz, C., J.H. Morrison, J.M. Wallace, J.A. Bonin, and J. Zhang, Arctic Ocean circulation patterns revealed by GRACE, *J. Climate*, *27*, 1445-1468, doi:10.1175/JCLI-D-13-00013.1, 2014 [published, refereed].

Schmidt, G. A., M. Kelley, L. Nazarenko, R. Ruedy, G. L. Russell, I. Aleinov, M. Bauer, S. Bauer, M. K. Bhat, R. Bleck, V. Canuto, Y. Chen, Y. Cheng, T. L. Clune, A. DelGenio, R. de Fainchtein, G. Faluvegi, J. E. Hansen, R. J. Healy, N. Y. Kiang, D. Koch, A. A. Lacis, A. N. LeGrande, J. Lerner, K. K. Lo, J. Marshall, E. E. Mathews, S. Menon, R. L. Miller, V. Oinas, A. Oloso, J. Perlwitz, M. J. Puma, W. M. Putman, D. Rind, A. Romanou, M. Sato, D. T. Shindell, S. Sun, R. Syed, N. Tausnev, K. Tsigaridis, N. Unger, A. Voulgarakis, M.-S. Yao, and J. Zhang, Configuration and assessment of the GISS ModelE2 contributions to the CMIP5 archive. *J. Advances in Modeling Earth Systems*, *6*, no. 2, 141-184, doi:10.1002/2013MS000265, 2014 [published, refereed].

Schweiger, A., and J. Zhang, Accuracy of short-term sea ice drift forecasts using a coupled ice–ocean model, *J. Geophy. Res*., *submitted*, 2015 [submitted, refereed].

Steele, M., S. Dickinson, and J. Zhang, Seasonal ice loss in the Beaufort Sea: Toward synchronicity and prediction, *J. Geophy. Res*., *120,* 1118-1132, doi: 10.1002/2014JC010247, 2015 [published, refereed].

Collow, T.W., W. Wang, A. Kumar, and J. Zhang, Improving Arctic sea ice prediction using PIOMAS initial sea ice thickness in a coupled ocean-atmosphere model, *Monthly Weather Review*, *submitted*, 2015 [published, refereed].

Zhang, J., R. Lindsay, A. Schweiger, and I. Rigor, Recent changes in the dynamic properties of declining Arctic sea ice: A model study, *Geophys. Res. Lett.*, *39*, L20503, doi:10.1029/2012GL053545, 2012 [published, refereed].

Zhang, J., R. Lindsay, A. Schweiger, and M. Steele, The impact of an intense summer cyclone on 2012 Arctic sea ice retreat, *Geophys. Res. Lett.*, *40*, doi:10.1002/grl.50190, 2013 [published, refereed].

Zhang, J., A. Schweiger, M. Steele, and H. Stern, Sea ice floe size distribution in the marginal ice zone: Theory and numerical experiments, *J. Geophys. Res.*, *120*, doi:10.1002/2015JC010770, 2015 [published, refereed].

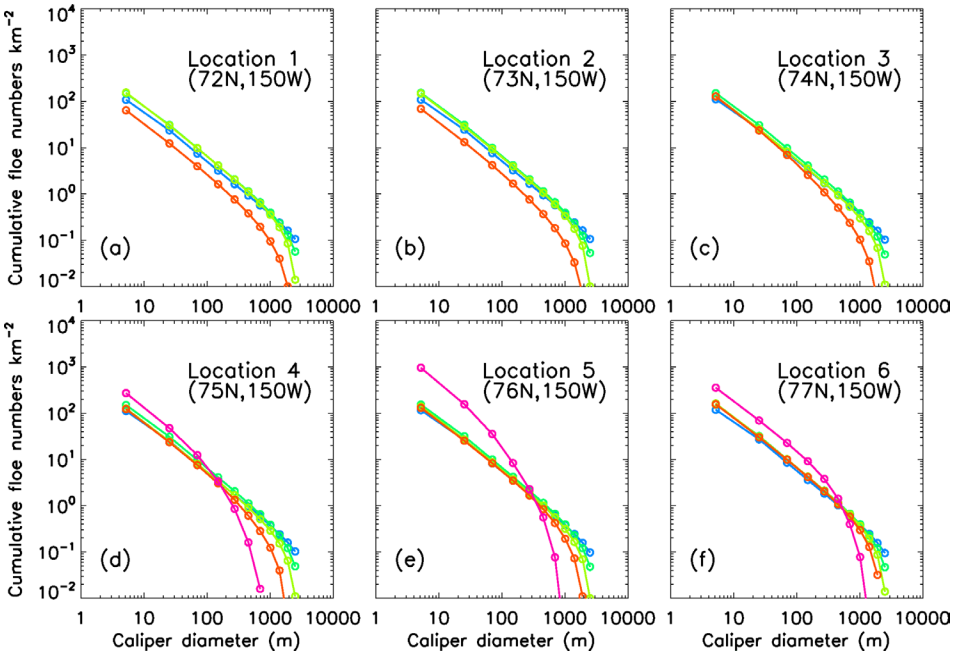

Figure 1. Log-log plots of some of the model simulated 2014 monthly mean cumulative FSD at six different latitudes along 150^{o}W in the Beaufort Sea. The model has 12 floe size categories, with floe size ranging from 0.1 m to ~3000 m. Blue color: May; green: June, green-yellow: July, red: August; pink: September. There is no pink curve in panels (a)–(c) because no ice is simulated at those locations in September 2014. The Zhang et al. (2015) FSD theory allows PIOMAS to obtain a cumulative FSD that always follows a power law, in space and time, as observed by satellites and aerial surveys. The simulated exponent of the power law, or the slope of the curves in the log-log plots, is also generally within the range of the observations (see Figure 2).

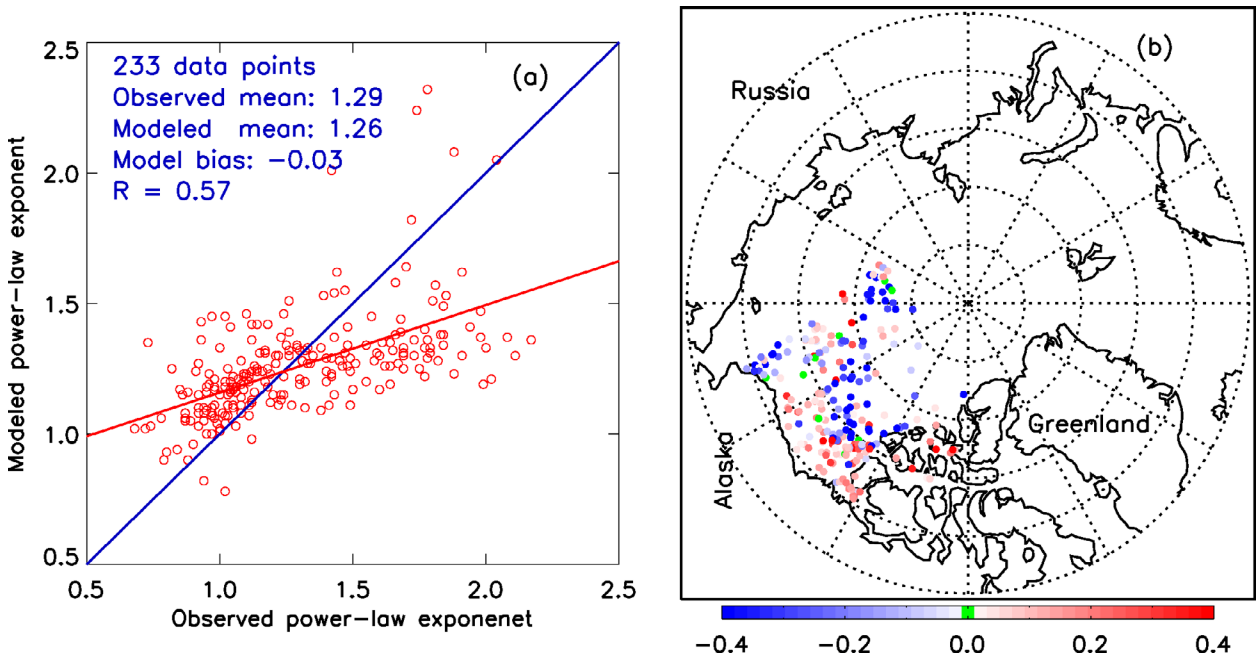

Figure 2. (a) A comparison with the power-law exponent of the cumulative FSD derived using MODIS images collected over April through October in 2013 and 2014. In (a) the blue line indicates equality and the red line represents the best fit to the observations. The number of total observation points, model and observation mean values, model bias (mean model-observation difference), and model-observation correlation (R) are listed. (b) Point-by-point power-law exponent differences between PIOMAS results and observations at the locations of the observations.

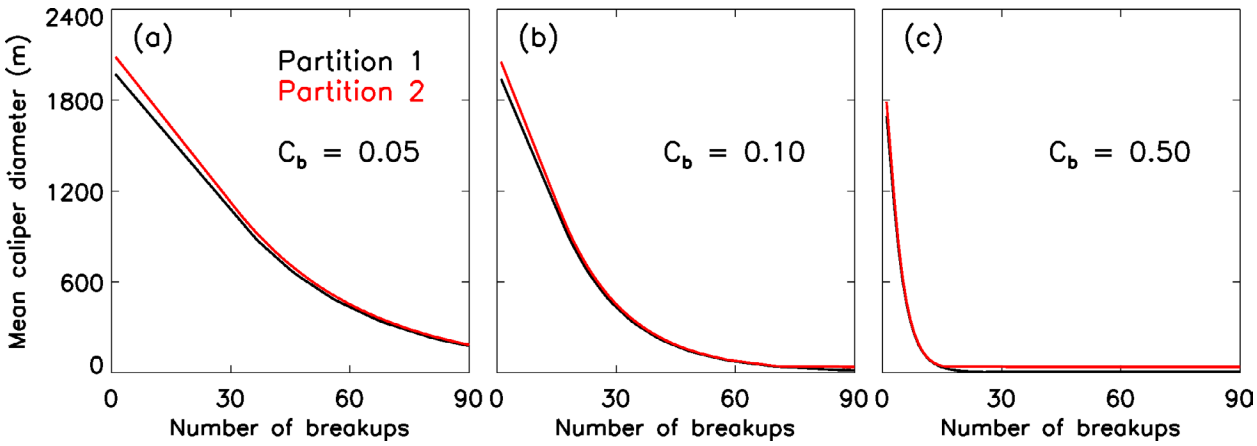

Figure 3. Changes in mean floe size (caliper diameter) in a succession of ice breakups, calculated using different floe size category partitions and participation factors of floe size redistribution. This figures shows that floe size redistribution and the resulting FSD and mean floe size do not, over a given floe size range such as 0.1–3000 m, depend on how floe size categories are numerically partitioned. This is an important feature, suggesting that the FSD theory is robust.

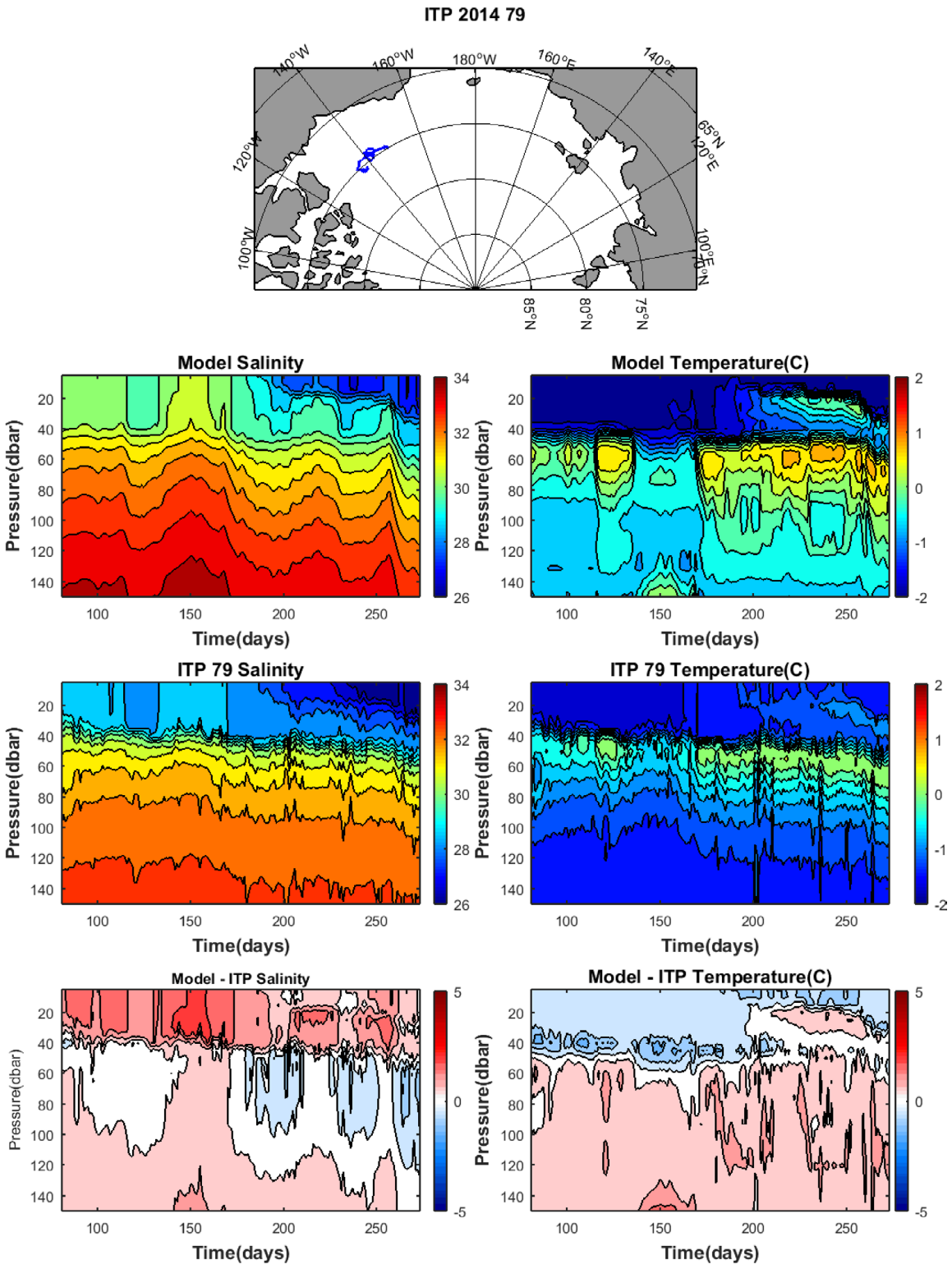

Figure 4. A comparison of 2014 ocean temperature and salinity profiles between MIZMAS and ice-tethered profiler #79. The panel in the top row shows the track of ITP79, the second row shows MIZMAS ocean temperature and salinity along the track, the third row shows ITP79 observations, and the bottom row shows differences between MIZMAS and ITP79.

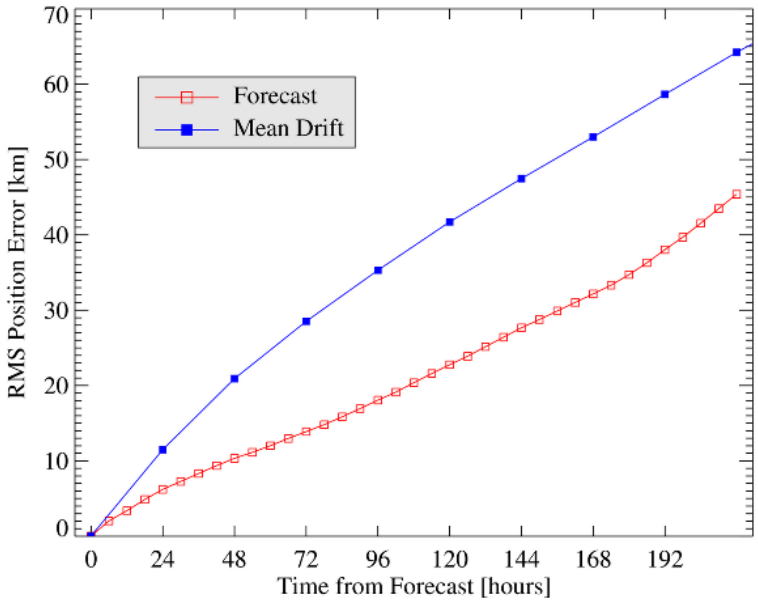

Figure 5. RMS position error at different forecast times for positions predicted by the MIZMAS forecast (red) and positions predicted by using mean daily velocity fields or climatology (blue).

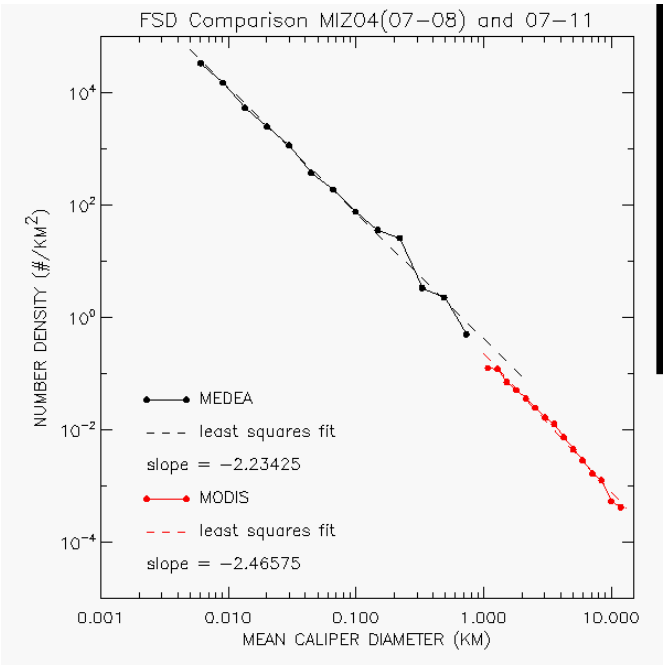

Figure 6. FSD from spatially overlapping MEDEA and MODIS images. MODIS images is from July 8, 2014, the corresponding MEDEA image is from July 11, 2014.

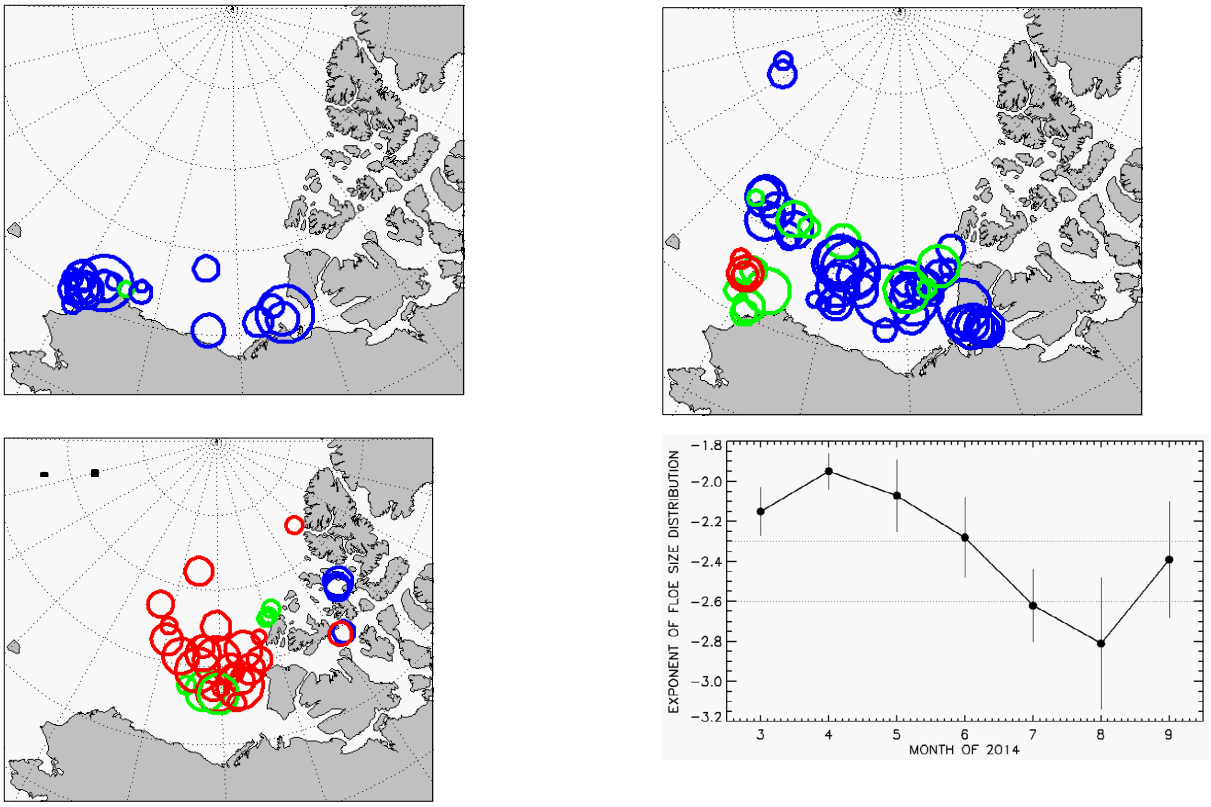

Figure 7 Slope of the MODIS-derived (non-cumulative) FSD for three time periods of 2014: March–April (upper left), May–June (upper right), and July–August (lower left). Blue circles indicate slopes less than –2.3, green circles indicate slopes between –2.3 and –2.6 and red circles show slopes steeper than -2.6. The seasonal cycle averaged from all the data is shown in the lower right panel.

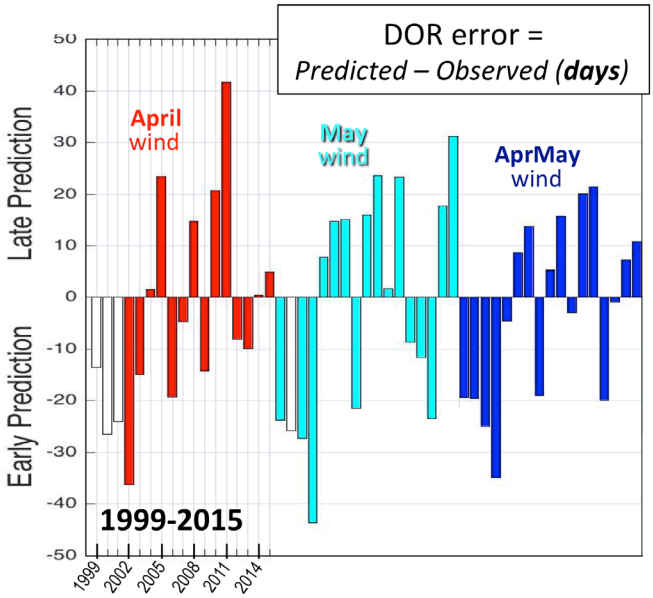

2003-2015	April only	May only	April and May
Prediction bias (days)	0	3	1.5
RMSE (days)	20	22	17
Correlation	0.46	0.44	0.58

Figure 8. (upper) Error in predicting the Date of ice Retreat (DOR) in the eastern Beaufort Sea by assuming a linear relationship between summer DOR and spring surface winds in April, in May, and in April+May. Winds from NCEP reanalysis, DOR from NSIDC passive microwave SSMI/SSMIS ice concentrations. Predictions improve with more years for training the linear relationship (i.e., in later years), and also with averaging over more spring days (i.e., April+May provides the best prediction). As in Steele et al. (2015), the eastern Beaufort Sea is here defined at 71°N along 120°W–135°W. (lower) Prediction bias, RMSE, and correlation.